Design Rules for High-Efficiency Quantum-Dot-Sensitized Solar Cells: A Multilayer Approach

ARTICLE *in* JOURNAL OF PHYSICAL CHEMISTRY LETTERS · AUGUST 2012

Impact Factor: 7.46 · DOI: 10.1021/jz3010078

4 AUTHORS, INCLUDING:

Menny Shalom
Max Planck Institute of Colloids and Interfaces
37 PUBLICATIONS **1,878** CITATIONS
SEE PROFILE

Arie Zaban
Bar Ilan University
170 PUBLICATIONS **10,725** CITATIONS
SEE PROFILE

THE JOURNAL OF PHYSICAL CHEMISTRY Letters

Letter

pubs.acs.org/JPCL

Design Rules for High-Efficiency Quantum-Dot-Sensitized Solar Cells: A Multilayer Approach

Menny Shalom, Sophia Buhbut, Shay Tirosh, and Arie Zaban*

Department of Chemistry, Center for Nanotechnology & Advanced Materials, Bar Ilan University, Ramat Gan 52900, Israel

Supporting Information

ABSTRACT: The effect of multilayer sensitization in quantum-dot (QD)-sensitized solar cells is reported. A series of electrodes, consisting of multilayer CdSe QDs were assembled on a compact TiO_2 layer. Photocurrent measurements along with internal quantum efficiency calculation reveal similar electron collection efficiency up to a 100 nm thickness of the QD layers. Moreover, the optical density and the internal quantum efficiency measurements reveal that the desired surface area of the TiO_2 electrode should be increased only by a factor of 17 compared with a compact electrode. We show that the sensitization of low-surface-area TiO_2 electrode with QD layers increases the performance of the solar cell, resulting in 3.86% efficiency. These results demonstrate a conceptual difference between the QD-sensitized solar cell and the dye-based system in which dye multilayer decreases the cell performance. The utilization of multilayer QDs opens new opportunities for a significant improvement of quantum-dot-sensitized solar cells via innovative cell design.

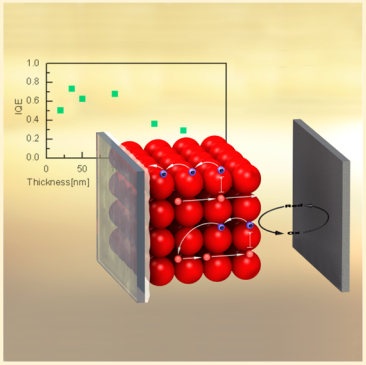

SECTION: Energy Conversion and Storage; Energy and Charge Transport

Quantum-dot-sensitized solar cells (QDSSCs) have been evolving rapidly over the last 2 years, resulting in a significant improvement of light to electric power conversion efficiencies, from 0.1% to ~6%.[1−5] The use of QDs as an absorber in the cell is motivated by the option of designing third-generation systems based on their tunable size-dependent properties,[6,7] including multiple carrier generation[8,9] (MEG), hot electron utilization,[10] and tandem cell configurations.[11,12] The operation of QDSSC is similar to the well-known dye-sensitized solar cell (DSSC).[13,14] Under illumination, photons are absorbed by the QDs, which inject the excited electrons into a wide bandgap semiconductor electrode while holes are transferred via the electrolyte to the back electrode.

The efficiency improvement in QDSSC may be attributed to both materials development and the progress in understanding the cell mechanisms. Materials development involves: (1) the emergence of absorbers such as PbS, PbSe, and Sb_2S_3, which extend the light absorption range from the visible to the near-infrared (NIR) region,[1,15−19] (2) the improvement of QD synthesis and loading using successive ionic layer adsorption and reaction[20−22] (SILAR), chemical bath deposition[23,24] (CBD) and electrophoretic deposition[25−27] (EPD), (3) different morphology of wide bandgap semiconductors,[18,28−31] (4) new counter electrodes,[32−35] and (5) the improvement of the redox couple electrolyte.[15,36−38] In addition to the materials development, efficiency increase is attributed to the basic understanding of the cell mechanisms including: (1) the existence of several electron injection paths, directly from the conduction band of the QD and via surface states,[28,39−41] (2) fast hole extraction relative to electron recombination with the electrolyte,[39,41] (3) charge accumulation in the QDs layer that modifies the electronic properties of the QD layer upon illumination,[41−43] and (4) the effect of surface modifications of both the QDs and the metal oxide that can reduce the recombination rates within the QDSSC.[44−48]

Recent improvements in QD synthesis and loading enable deposition of QD multilayer on the porous, wide bandgap semiconductor electrode. While offering the desired increase in optical density per electrode area, by analogy to DSSC in which the dye multilayer reduces the performance of the cell, QDs multilayer configuration is frequently considered to be inefficient. It is often assumed that the QD multilayer enhances recombination from the QDs to the electrolyte mostly due to low charge conductivity within the QDs layer.[40] Here we report a systematic study showing that up to a given thickness the QD multilayer can increase the efficiency of QDSSCs. The measured improvement in cell performance results from a higher quantum yield of charge separation at a cretin multilayer range and from the ability to reduce the thickness of the porous electrode due to the very high absorption cross-section of the QDs multilayer. Consequently, we suggest new design rules for high-efficiency QDSSCs.

Direct measurements of the correlation between the QD multilayer thickness and cell performance were made by utilizing compact QDSSCs. The compact configuration avoids the ambiguity associated with porosity decline upon QD growth inside the pores and the possible nonuniformity of the QD layer resulting from the rough electrode morphology. The

Received: July 22, 2012
Accepted: August 17, 2012
Published: August 21, 2012

dx.doi.org/10.1021/jz3010078 | J. Phys. Chem. Lett. 2012, 3, 2436−2441

cell consisted of a QD-sensitized TiO_2 photoanode, polysulfide electrolyte (1 M Na_2S/0.1 M S), and a PbS counter electrode[34] (Figure 1). The photoanode was fabricated by spry pyrolysis of

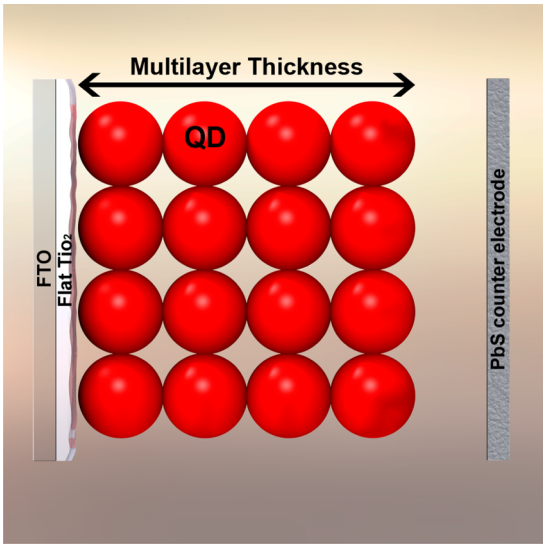

Figure 1. Schematic drawing of QDSSC consisting of multilayer quantum dots (varied in thickness) that are deposited directly on compact TiO_2 electrode.

compact TiO_2 (~180 nm thick) over a conductive glass (FTO), followed by CBD of a CdSe QDs multilayer with the following properties: (1) sizewise polydispersed QDs, (2) good electrical contact to the TiO_2 because of the direct growth method, and (3) deposition time determining the multilayer thickness while affecting the size of the QDs.

Figure 2 presents HRSEM cross-section images of six similar photo anodes that differ by the CdSe deposition duration. The QDs layers are marked by white arrows. The thickness of the QDs multilayer formed on the compact TiO_2 varied from 20 nm for short deposition to 190 nm for the longest deposition duration. The optical density of the six electrodes corresponds well to the thickness of the QDs sensitizer (absorption spectra provided in Figure S1 of the Supporting Information). The red shift of the absorption onset indicates that growth duration also involves an increase in the average QDs size.

The photocurrents obtained from the six electrodes with respect to the thickness of the QDs multilayer are presented in Figure 3. An increase in the QDs layer thickness results in

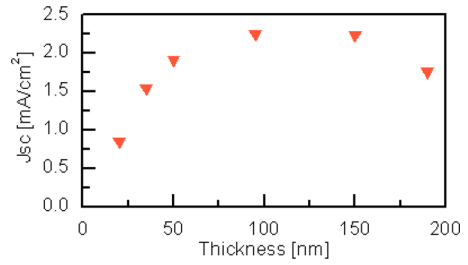

Figure 3. Photocurrent density as a function of thickness of the QDs multilayer deposited on compact TiO_2 electrodes.

higher photocurrents of up to 2.3 mA/cm^2 at ~100 nm, after which further QD deposition reduces the photocurrent. External quantum efficiency (EQE) measurements, which correlate well with the absorption spectra of the electrodes (including the red shift of the current onset), show a similar trend (Figure S2 of the Supporting Information).

The photocurrent in QDSSCs is affected by several parameters that define a set of efficiencies for the various processes occurring under illumination: light absorption, charge separation into the TiO_2 and the electrolyte, charge collection via the two phases (QDs and TiO_2) and various recombination processes across the cell. Having changed only the thickness of the QD layer, we assign the photocurrent variations presented in Figure 3 to two main factors: (1) the optical density of the QDs layer, which defines the number of photons absorbed by the sensitizer and (2) the electron diffusion length across the QDs layer, which is a product of the lifetime and diffusion rate of the electron within the QD layer. While thicker QD layers lead to higher photocurrents by absorbing more of the incident photons, an opposite effect arises from the longer diffusion distance of the photogenerated electrons across the QD layer. One can normalize the optical density effect by calculating the internal quantum efficiency (IQE = EQE/absorbance),

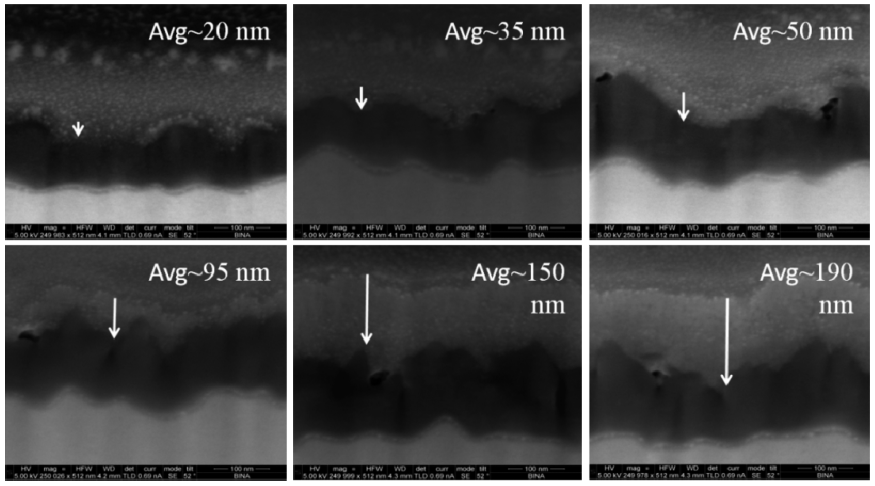

Figure 2. HRSEM images of six multilayer photo anodes. The white arrow highlights the thickness variation of the QDs layer (20–190 nm), which is deposited on compact TiO_2 (average thickness of 180 nm)-FTO glass. Scale bar for all images is 100 nm. The bottom layer (white) is the FTO glass, followed by the TiO_2 layer (black) and the QDs (gray, marked by the arrow).

dx.doi.org/10.1021/jz3010078 | J. Phys. Chem. Lett. 2012, 3, 2436–2441

providing an estimation for the electron diffusion length across the QDs multilayer.

Figure 4 presents the white-light IQE of the six cells as a function of the QDs multilayer thickness. White-light IQE is

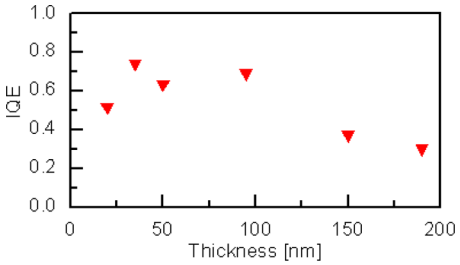

Figure 4. White-light IQE (internal quantum yield, measured electron per absorbed photon) as a function of the QDs multilayer thickness (compact TiO_2 electrodes), showing a plateau in efficiency of up to ~100 nm.

calculated by dividing the measured photocurrent by the maximum theoretical value of each cell. The maximum theoretical current is the product of the spectral absorbance of each cell and the wavelength-dependent photon flux of the illumination source, integrated over the photoactive region. Figure 4 reveals a plateau of the white-light IQE in the first 100 nm of QDs thicknesses, presenting values of 0.7 to 0.8, which significantly decrease for thicker QD layers. Consequently, the diffusion length within the CdSe QDs layer is sufficiently large to allow the collection of photogenerated electrons up to 100 nm away from the compact TiO_2. Electrons generated beyond ~100 nm do not contribute to the overall current and are lost to recombination processes before reaching the TiO_2 substrate as evident from the photocurrent measurements (Figure 3) and the calculated IQE (Figure 4). Within the general understanding of the ability to use multi-QD-layers as sensitizers, we note that the specific thickness of ~100 nm stands for CdSe QDs deposited by CBD. The optimal value for other materials or deposition methods is expected to vary.

The results presented in Figure 4 indicate one of the critical differences between QDSSCs and their analogues, the DSSCs. Whereas in the latter only dyes that are directly attached to the TiO_2 exhibit efficient sensitization, in QDSSCs, multilayer sensitization is effective. Consequently, the optical density per TiO_2 unit area in QDSSCs can be significantly higher than that of DSSC, thus allowing the use of a lower surface area TiO_2 electrode, which opens the ability to reduce recombination losses within the cell.

It is well known that recombination in these cells declines when the electrodes are made thinner, provided that the porosity allows fast diffusion of the redox mediator. Electrons generated within 4 μm away from the TiO_2 electrode have almost 100% collection efficiency as long as the oxidized ions transferring the holes to the back electrode are not trapped within the porous structure due to slow diffusion. As shown below, we calculate the surface area required for two CdSe QD sensitizer thicknesses to provide values for the design of the optimal TiO_2 electrode. We follow by measurements that validate the calculated optimization of the TiO_2 surface area. Finally, we suggest a new configuration for the TiO_2 electrode, aiming at efficiency and porosity that will be suitable for a large variety of hole conductors including solid-state systems.

The required TiO_2 surface area is calculated for two of the compact electrodes presented above, both sensitized by CdSe QDs with layer thicknesses of 35 and 100 nm. The calculation is expressed in terms of surface area factor (SA_f), representing the ratio between the TiO_2 surface area and the projected area (glass substrate). Multiplying the absorption spectrum of a compact electrode by a SA_f provides the expected cell spectrum from which one can calculate the fraction of incident photons absorbed by the sensitizer and the integration over the spectral window of the cell. The photon absorption fractions per SA_f for the two compact electrodes are presented in Figure 5. To

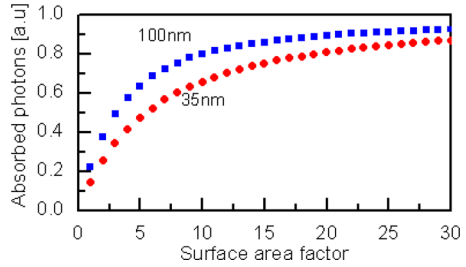

Figure 5. Fraction of incident photon absorbed in the 100 (blue square) and 35 nm (red square) QDs multilayer electrodes as a function of surface area factor.

absorb 90% of the solar photons that match the spectral window of the cell, the SA_f varies from 17 to 30 for the 100 nm to the 35 nm thick layers of the CdSe QDs sensitizer. These values are significantly lower than the 1000–2000 factor used in efficient DSSCs. Consequently, one can design a very thin photoanode for the QDSSC while maintaining large pores for the electrolyte.

To examine this approach, we inspected the performance of TiO_2 electrodes fabricated from large particles (average size 120 nm). The use of large particles creates a mesoporous structure with pore sizes in the range of 80–140 nm, which allow the deposition of multilayer QDs within the pores up to a thickness of ~60 nm. The *I*–*V* characteristics of the multilayer cell under simulated 1 Sun (Figure 6) demonstrate an impressive

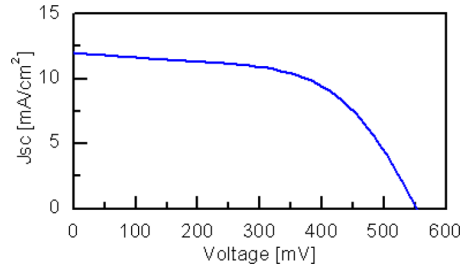

Figure 6. *I*–*V* characteristics of CdSe QD-sensitized solar cell based on multilayer QDs deposited onto large TiO_2 particles.

efficiency of 3.86% (V_{oc} = 556 mV, J_{sc} = 12 mA/cm^2, FF = 58%) despite two critical limitations associated with the electrode geometry: (1) strong scattering of the incoming radiation due to the size of the TiO_2 nanocrystals and (2) the nonuniform thickness of the QD sensitizer layer.

In the final section, we suggest a new design for the TiO_2 electrode that will enable the deposition of a thick, uniform sensitizer layer without scattering at the TiO_2–glass interface. The new design is motivated by the efficiency obtained with the 120 nm TiO_2 particle electrode in conjunction with the high

dx.doi.org/10.1021/jz3010078 | *J. Phys. Chem. Lett.* 2012, 3, 2436–2441

IQE values of this system (as follows). The EQE spectrum of the QD-sensitized, large TiO_2 electrode is presented in Figure 7a together with the corresponding compact electrode result.

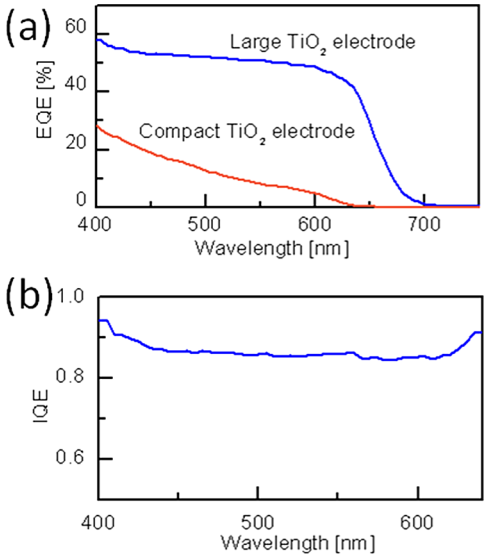

Figure 7. (a) EQE (external quantum efficiency) measurement of the multilayer QDs (~100 nm thickness) deposited on compact TiO_2 (red curve) and on large TiO_2 particles (blue curve). (b) IQE (internal quantum efficiency) of the multilayer QDs on large TiO_2 particles.

Both spectra correlated with their absorption spectra (Supporting Information, Figure S3). As expected, the increase in TiO_2 surface area associated with the porous geometry improves the EQE throughout the spectral response window of the cell, especially toward the absorption edge where the extinction coefficient of the QDs is low. Calculation of the IQE spectrum (Figure 7b) reveals remarkably high values, around 0.9 throughout the spectral response window, indicating that at least 90% of the absorbed photons drive charge separation, whereas a similar value stands for the fraction of QDs that contribute to the total photocurrent. Consequently, electrode geometry that reduces the scattering while maintaining the space required for the application of ~100 nm of QD sensitizer should achieve 90% conversion of the incident radiation to photocurrent (within the spectral response window of the QDs).

On the basis of the design rules described above, we suggest the geometry presented in Figure 8 for the TiO_2 electrode of QDSSCs. The specific dimensions stand for the studied system, that is, CdSe QDs deposited by CBD. Other QD materials or deposition methods will require adjustment of the electrode dimensions based on the specific properties of the QDs layer. The optimal electrode should consist of vertically aligned, 80 nm in diameter, TiO_2 nanorods deposited in hexagonal geometry. The nanorods should be spaced from each other by a distance of larger than 250 nm to allow the uniform growth of a ~100 nm thick QDs layer. A scattering layer in the form of large wide bandgap powder can be added on top of the nanorods. Under these conditions, over 90% of the incident photons can be absorbed by a nanorods layer, thinner than 3 μm, which should have a positive effect on both the photocurrent and the photovoltage of the cell. Furthermore, the combination of standing rods geometry and the low aspect

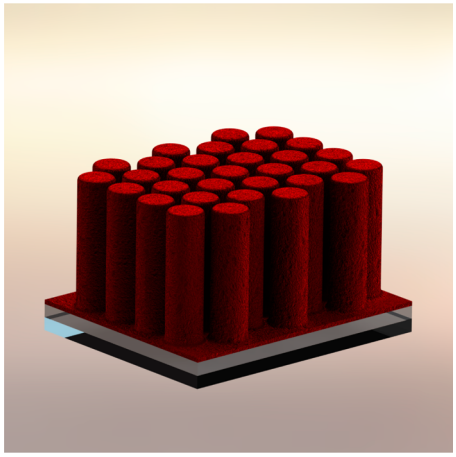

Figure 8. Illustration of the optimal TiO_2 electrode structure for QDSSC. The electrode should consist of vertically aligned TiO_2 nanorods (80 nm in diameter) deposited with a hexagonal geometry. The nanorods should have a spacing larger than 250 nm between each to allow the uniform growth of a ~100 nm thick QDs layer.

ratio of the resulting pores should enable good infiltration of a solid-state hole mediator such as conducting polymers.[1]

The design can tolerate variation in rod diameter (50–250 nm) and in distance between the rods (200–300 nm). Such variations can be compensated by the elongation of the nanorods up to 4 μm, a length at which electron collection and open circuit recombination may be affected. Our effort to fabricate such structures on the large scale needed for real devices will be reported later.

In this work, we demonstrate the ability to assemble a multilayer of QDs as sensitizers in a quantum-dot-sensitized solar cell. IQE measurements combined with the surface-area-factor calculations show optimal multilayer QDs thickness of 100 nm. Consequently, our results indicate that there is no need for a high-surface-area electrode for QDSSC as commonly used. We have shown that the use of multilayer QDs that were deposited onto large porous (low surface area) TiO_2 increases the performance of the solar cell, resulting in 3.86% efficiency. The utilization of a multilayer sensitizer opens new opportunities for the significant improvement of QDSSCs via innovative cell design.

■ EXPERIMENTAL DATA

CdSe QD-sensitized solar cell was fabricated by using the following: (1) Commercial TiO_2 paste (Ti–Nanoxide D, Solaronix, Switzerland) made by the doctor blade technique on fluorine-doped tin oxide (FTO) and sintered at 450 °C for 30 min. (2) Dense compact layers prepared by spray pyrolysis on FTO covered glass substrates at 450 °C using compressed air as a carrier gas. The mesoporous film thickness was 7.8 μm, measured by a profile-meter (Surftest SV-500). For the CdSe multilayer deposition, a seeding layer of CdS was deposited by the SILAR method prior to the CdSe sensitization. Therefore, the TiO_2 electrodes were dipped into 0.1 M $Cd(ClO_4)_2$ for 1 min, washed with deionized water, immersed into 0.1 M Na_2S aqueous solution, and washed again.[21] After seeding, CBD was used to sensitize the electrode with CdSe QDs, following the procedure by Gorer and Hodes.[49] Sodium selenosulphate (Na_2SeSO_3) solution (80 mM) was prepared by dissolving Se powder in a 200 mM Na_2SO_3 solution (solution A). $CdSO_4$ (80 mM) and trisodiumsalt of nitrilotriacetic acid (N-

dx.doi.org/10.1021/jz3010078 | J. Phys. Chem. Lett. 2012, 3, 2436–2441

$(CH_2COONa)_3$) (120 mM) were mixed in a volume ratio 1:1 (solution B) before solutions A and B were mixed in a volume ratio 1:2. The TiO_2 electrodes were immersed into the final solution for 5−50 h at 10 °C and kept in the dark. Photocurrent voltage characteristics were performed with an Eco-Chemie potentiostat. A solar simulator class A (new port) calibrated to 100 mW/cm^2 (AM 1.5 spectrum) served as a light source. The illuminated area of the cell was set to 1.03 cm^2 using an aperture. Na_2S (1 M), 0.1 M sulfur, and 0.1 M KOH solution served as the electrolyte. A PbS foil was used as a counter-electrode. A 250 W xenon arc lamp (Oriel) served as a light source for incident photon to current efficiency (IPCE). The absorption spectra of the multilayer electrodes were measured using a Varian spectrophotometer equipped with an integrating sphere. A cross section of the electrodes was performed using a Helios 600, dual beam scanning electron microscopy (SEM), and focus ion beam (FIB) instrument.

■ ASSOCIATED CONTENT

Supporting Information

Absorption spectra and the EQE of the CdSe multilayer-based solar cells: on compact and mesoporous TiO_2. This material is available free of charge via the Internet at http://pubs.acs.org.

■ AUTHOR INFORMATION

Corresponding Author

*E-mail: zabana@mail.biu.ac.il.

Notes

The authors declare no competing financial interest.

■ ACKNOWLEDGMENTS

We thank the Israel Ministry of Science, Tshtiyot Program, for the financial support. Menny Shalom thanks the "Converging Technologies" program.

■ REFERENCES

(1) Boix, P. P.; Lee, Y. H.; Fabregat-Santiago, F.; Im, S. H.; Mora-Sero, I.; Bisquert, J.; Seok, S. I. From Flat to Nanostructured Photovoltaics: Balance between Thickness of the Absorber and Charge Screening in Sensitized Solar Cells. *ACS Nano* **2012**, *6*, 873−880.

(2) Im, S. H.; Lim, C. S.; Chang, J. A.; Lee, Y. H.; Maiti, N.; Kim, H. J.; Nazeeruddin, M. K.; Gratzel, M.; Seok, S. I. Toward Interaction of Sensitizer and Functional Moieties in Hole-Transporting Materials for Efficient Semiconductor-Sensitized Solar Cell. *Nano Lett.* **2011**, *11*, 4789−4793.

(3) Santra, P. K.; Kamat, P. V. Mn-Doped Quantum Dot Sensitized Solar Cells: A Strategy to Boost Efficiency over 5%. *J. Am. Chem. Soc.* **2012**, *134*, 2508−2511.

(4) Vogel, R.; Hoyer, P.; Weller, H. Quantum-Sized PbS, CdS, Ag_2S, Sb_2S_3, and Bi_2S_3 Particles as Sensitizers for Various Nanoporous Wide-Bandgap Semiconductor. *J. Phys. Chem.* **1994**, *98*, 3183−3188.

(5) Zaban, A.; Micic, O. I.; Gregg, B. A.; Nozik, A. J. Photosensitization of Nanoporous TiO_2 Electrodes with InP Quantum Dots. *Langmuir* **1998**, *14*, 3153−3156.

(6) Kamat, P. V. Quantum Dot Solar Cells. Semiconductor Nanocrystals as Light Harvesters. *J. Phys. Chem. C.* **2008**, *112*, 18737−18753.

(7) Ruhle, S.; Shalom, M.; Zaban, A. Quantum Dot Sensitized Solar Cells. *Chem. Phys. Chem.* **2010**, *11*, 2290−2304.

(8) Nozik, A. J. Photovoltaics Separating Multiple Exciton. *Nat. Photonics.* **2012**, *6*, 272−273.

(9) Semonin, O. E.; Luther, J. M.; Choi, S.; Chen, H. Y.; Gao, J. B.; Nozik, A. J.; Beard, M. C. Peak External Photocurrent Quantum Efficiency Exceeding 100% via MEG in a Quantum Dot Solar Cell. *Science* **2011**, *334*, 1530−1533.

(10) Tisdale, W. A.; Williams, K. J.; Timp, B. A.; Norris, D. J.; Aydil, E. S.; Zhu, X. Y. Hot-Electron Transfer from Semiconductor Nanocrystals. *Science* **2010**, *328*, 1543−1547.

(11) Shalom, M.; Hod, I.; Tachan, Z.; Buhbut, S.; Tirosh, S.; Zaban, A. Quantum Dot Based Anode and Cathode for High Voltage Tandem Photo-Electrochemical Solar Cell. *Energy Environ. Sci.* **2011**, *4*, 1874−1878.

(12) Wang, X. H.; Koleilat, G. I.; Tang, J.; Liu, H.; Kramer, I. J.; Debnath, R.; Brzozowski, L.; Barkhouse, D. A. R.; Levina, L.; Hoogland, S.; Sargent, E. H. Tandem Colloidal Quantum Dot Solar Cells Employing a Graded Recombination Layer. *Nat. Photonics.* **2011**, *5*, 480−484.

(13) Gratzel, M. Dye Sensitized Solar Cells. *J. Photochem. Photobiol., C.* **2003**, *4*, 145−153.

(14) Hagfeldt, A.; Boschloo, G.; Sun, L. C.; Kloo, L.; Pettersson, H. Dye Sensitized Solar Cells. *Chem. Rev.* **2010**, *110*, 6595−6663.

(15) Boix, P. P.; Larramona, G.; Jacob, A.; Delatouche, B.; Mora-Sero, I.; Bisquert, J. Hole Transport and Recombination in All Solid Sb_2S_3 Sensitized TiO_2 Solar Cells Using CuSCN As Hole Transporter. *J. Phys. Chem. C.* **2012**, *116*, 1579−1587.

(16) Im, S. H.; Kim, H. J.; Kim, S. W.; Seok, S. I. All Solid State Multiply Layered PbS Colloidal Quantum Dot Sensitized Photovoltaic Cells. *Energy Environ. Sci.* **2011**, *4*, 4181−4186.

(17) Yang, Y.; Rodriguez-Cordoba, W.; Xiang, X.; Lian, T. Q. Strong Electronic Coupling and Ultrafast Electron Transfer between PbS Quantum Dots and TiO_2 Nanocrystalline Films. *Nano Lett.* **2012**, *12*, 303−309.

(18) Dittrich, T.; Belaidi, A.; Ennaoui, A. Concepts of Inorganic Solid State Nanostructured Solar Cells. *Sol. Energy Mater. Sol. Cells* **2011**, *95*, 1527−1536.

(19) Zhao, N.; Osedach, T. P.; Chang, L. Y.; Geyer, S. M.; Wanger, D.; Binda, M. T.; Arango, A. C.; Bawendi, M. G.; Bulovic, V. Colloidal PbS Quantum Dot Solar Cells with High Fill Factor. *ACS Nano* **2010**, *4*, 3743−3752.

(20) Gonzalez-Pedro, V.; Xu, X. Q.; Mora-Sero, I.; Bisquert, J. Modeling High Efficiency Quantum Dot Sensitized Solar Cells. *ACS Nano* **2010**, *4*, 5783−5790.

(21) Zewdu, T.; Clifford, J. N.; Hernandez, J. P.; Palomares, E. Photo Induced Charge Transfer Dynamics in Efficient TiO_2/CdS/CdSe Sensitized Solar Cells. *Energy Environ. Sci.* **2011**, *4*, 4633−4638.

(22) Mora-Sero, I.; Bisquert, J. Breakthroughs in the Development of Semiconductor Sensitized Solar Cells. *J. Phys. Chem. Lett.* **2010**, *1*, 3046−3052.

(23) Hodes, G. Semiconductor and Ceramic Nanoparticle Films Deposited by Chemical Bath Deposition. *Phys. Chem. Chem. Phys.* **2007**, *9*, 2181−2196.

(24) Kokotov, M.; Hodes, G. Influence of Selective Nucleation on the One Step Chemical Bath Deposition of CdS/ZnO and CdS/ZnS Composite Films. *Chem. Mater.* **2010**, *22*, 5483−5491.

(25) Brown, P.; Kamat, P. V. Quantum Dot Solar Cells - Electrophoretic deposition of CdSe-C-60 Composite Films and Capture of Photogenerated Electrons with nC(60) Cluster Shell. *J. Am. Chem. Soc.* **2008**, *130*, 8890−8891.

(26) Salant, A.; Shalom, M.; Hod, I.; Faust, A.; Zaban, A.; Banin, U. Quantum Dot Sensitized Solar Cells with Improved Efficiency Prepared Using Electrophoretic Deposition. *ACS Nano* **2010**, *4*, 5962−5968.

(27) Salant, A.; Shalom, M.; Tachan, Z.; Buhbut, S.; Zaban, A.; Banin, U. Quantum Rod Sensitized Solar Cell: Nanocrystal Shape Effect on the Photovoltaic Properties. *Nano Lett.* **2012**, *12*, 2095−2100.

(28) Tvrdy, K.; Frantsuzov, P. A.; Kamat, P. V. Photoinduced Electron Transfer from Semiconductor Quantum Dots to Metal Oxide Nanoparticles. *Proc. Natl. Acad. Sci. U.S.A.* **2011**, *108*, 29−34.

(29) Barcelo, I.; Lana-Villarreal, T.; Gomez, R. Efficient Sensitization of ZnO Nanoporous Films with CdSe QDs Grown by Successive Ionic Layer Adsorption and Reaction (SILAR). *J. Photochem. Photobiol., A* **2011**, *220*, 47−53.

(30) Canovas, E.; Moll, P.; Jensen, S. A.; Gao, Y. A.; Houtepen, A. J.; Siebbeles, L. D. A.; Kinge, S.; Bonn, M. Size Dependent Electron

Transfer from PbSe Quantum Dots to SnO_2 Monitored by Picosecond Terahertz Spectroscopy. *Nano Lett.* **2011**, *11*, 5234−5239.
(31) Sudhagar, P.; Song, T.; Lee, D. H.; Mora-Sero, I.; Bisquert, J.; Laudenslager, M.; Sigmund, W. M.; Park, W. I.; Paik, U.; Kang, Y. S. High Open Circuit Voltage Quantum Dot Sensitized Solar Cells Manufactured with ZnO Nanowire Arrays and Si/ZnO Branched Hierarchical Structures. *J. Phys. Chem. Lett.* **2011**, *2*, 1984−1990.
(32) Paul, G. S.; Kim, J. H.; Kim, M. S.; Do, K.; Ko, J.; Yu, J. S. Different Hierarchical Nanostructured Carbons as Counter Electrodes for CdS Quantum Dot Solar Cells. *ACS Appl. Mater. Interfaces* **2012**, *4*, 375−381.
(33) Radich, J. G.; Dwyer, R.; Kamat, P. V. Cu_2S Reduced Graphene Oxide Composite for High Efficiency Quantum Dot Solar Cells. Overcoming the Redox Limitations of S_2^-/S_n^{2-} at the Counter Electrode. *J. Phys. Chem. Lett.* **2011**, *2*, 2453−2460.
(34) Tachan, Z.; Shalom, M.; Hod, I.; Ruhle, S.; Tirosh, S.; Zaban, A. PbS as a Highly Catalytic Counter Electrode for Polysulfide Based Quantum Dot Solar Cells. *J. Phys. Chem. C.* **2011**, *115*, 6162−6166.
(35) Shengyuan, Y.; Nair, A. S.; Peining, Z.; Ramakrishna, S. Electrospun TiO_2 Nanostructures Sensitized by CdS in Conjunction with CoS Counter Electrodes: Quantum Dot Sensitized Solar Cells All Prepared by Successive Ionic Layer Adsorption and Reaction. *Mater. Lett.* **2012**, *76*, 43−46.
(36) Chakrapani, V.; Baker, D.; Kamat, P. V. Understanding the Role of the Sulfide Redox Couple (S^{2-}/S_n^{2-}) in Quantum Dot-Sensitized Solar Cells. *J. Am. Chem. Soc.* **2011**, *133*, 9607−9615.
(37) Jovanovski, V.; Gonzalez-Pedro, V.; Gimenez, S.; Azaceta, E.; Cabanero, G.; Grande, H.; Tena-Zaera, R.; Mora-Sero, I.; Bisquert, J. A Sulfide/Polysulfide Based Ionic Liquid Electrolyte for Quantum Dot Sensitized Solar Cells. *J. Am. Chem. Soc.* **2011**, *133*, 20156−20159.
(38) Ning, Z. J.; Yuan, C. Z.; Tian, H. N.; Fu, Y.; Li, L.; Sun, L. C.; Agren, H. Type-II Colloidal Quantum Dot Sensitized Solar Cells with a Thiourea Based Organic Redox Couple. *J. Mater. Chem.* **2012**, *22*, 6032−6037.
(39) Guijarro, N.; Shen, Q.; Gimenez, S.; Mora-Sero, I.; Bisquert, J.; Lana-Villarreal, T.; Toyoda, T.; Gomez, R. Direct Correlation between Ultrafast Injection and Photoanode Performance in Quantum Dot Sensitized Solar Cells. *J. Phys. Chem. C* **2010**, *114*, 22352−22360.
(40) Hodes, G. Comparison of Dye and Semiconductor Sensitized Porous Nanocrystalline Liquid Junction Solar Cells. *J. Phys. Chem. C* **2008**, *112*, 17778−17787.
(41) Shalom, M.; Tachan, Z.; Bouhadana, Y.; Barad, H. N.; Zaban, A. Illumination Intensity Dependent Electronic Properties in Quantum Dot Sensitized Solar Cells. *J. Phys. Chem. Lett.* **2011**, *2*, 1998−2003.
(42) Zillner, E.; Dittrich, T. Surface Photovoltage within a Monolayer of CdSe Quantum Dots. *Phys. Status Solidi RRL* **2011**, *5*, 256−258.
(43) Hod, I.; Gonzalez-Pedro, V.; Tachan, Z.; Fabregat-Santiago, F.; Mora-Sero, I.; Bisquert, J.; Zaban, A. Dye versus Quantum Dots in Sensitized Solar Cells: Participation of Quantum Dot Absorber in the Recombination Process. *J. Phys. Chem. Lett.* **2011**, *2*, 3032−3035.
(44) Albero, J.; Martinez-Ferrero, E.; Iacopino, D.; Vidal-Ferran, A.; Palomares, E. Interfacial Charge Transfer Dynamics in CdSe/Dipole Molecules Coated Quantum Dot Polymer Blends. *Phys. Chem. Chem. Phys.* **2010**, *12*, 13047−13051.
(45) Mora-Sero, I.; Gimenez, S.; Fabregat-Santiago, F.; Gomez, R.; Shen, Q.; Toyoda, T.; Bisquert, J. Recombination in Quantum Dot Sensitized Solar Cells. *Acc. Chem. Res.* **2009**, *42*, 1848−1857.
(46) Shalom, M.; Ruhle, S.; Hod, I.; Yahav, S.; Zaban, A. Energy Level Alignment in CdS Quantum Dot Sensitized Solar Cells Using Molecular Dipoles. *J. Am. Chem. Soc.* **2009**, *131*, 9876−9877.
(47) Shen, Q.; Kobayashi, J.; Diguna, L. J.; Toyoda, T. Effect of ZnS Coating on the Photovoltaic Properties of CdSe Quantum Dot Sensitized Solar Cells. *J. Appl. Phys.* **2008**, *103*, 084304−084309.
(48) Barea, E. M.; Shalom, M.; Gimenez, S.; Hod, I.; Mora-Sero, I.; Zaban, A.; Bisquert, J. Design of Injection and Recombination in Quantum Dot Sensitized Solar Cells. *J. Am. Chem. Soc.* **2010**, *132*, 6834−6839.
(49) Gorer, S.; Hodes, G. Quantum Size Effects in the Study of Chemical Solution Deposition Mechanisms of Semiconductor Films. *J. Phys. Chem.* **1994**, *98*, 5338−5346.